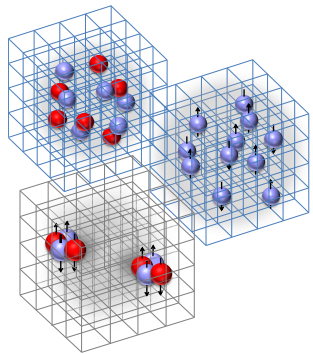


Overview from Nuclear Lattice Effective Field Theory

Serdar Elhatisari

Nuclear Lattice EFT Collaboration
HISKP, Universität Bonn

Workshop on
Polarized light ion physics with EIC
Ghent University, Belgium
February 5-9, 2018



Nuclear Lattice Effective Field Theory collaboration

Serdar Elhatisari (Bonn)

Evgeny Epelbaum (Bochum)

Nico Klein (Bonn)

Hermann Krebs (Bochum)

Timo Lähde (Jülich)

Dean Lee (MSU)

Ning Li (MSU)

Bing-Nan Lu (MSU)

Thomas Luu (Jülich)

Ulf-G. Meißner (Bonn/Jülich)

Gautam Rupak (MSU)

Gianluca Stellin (Bonn)



Bundesministerium
für Bildung
und Forschung



Deutsche
Forschungsgemeinschaft
DFG



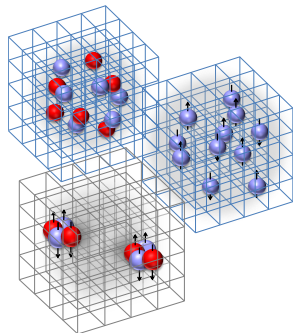
European Research Council
Established by the European Commission
Supporting top researchers
from anywhere in the world

 HELMHOLTZ
GEMEINSCHAFT



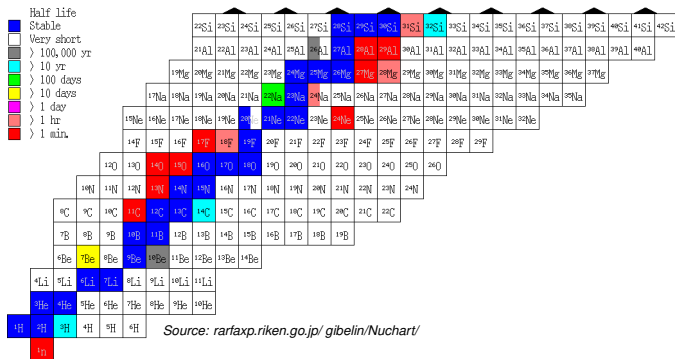
Outline

- Introduction
- Lattice effective field theory
- *Adiabatic projection method*:
scattering and reactions on the lattice
- Degree of locality of nuclear forces
- *Nuclear clusters*:
probing for alpha clusters
- *Pinhole Algorithm*:
density profiles for nuclei
- Summary



Ab initio nuclear structure and nuclear scattering

□ nuclear structure :



□ nuclear scattering : ... processes relevant for stellar astrophysics

- ▷ scattering of alpha particles : ${}^4\text{He} + {}^4\text{He} \rightarrow {}^4\text{He} + {}^4\text{He}$
- ▷ triple-alpha reaction : ${}^4\text{He} + {}^4\text{He} + {}^4\text{He} \rightarrow {}^{12}\text{C} + \gamma$
- ▷ alpha capture on carbon : ${}^4\text{He} + {}^{12}\text{C} \rightarrow {}^{16}\text{O} + \gamma$

⋮

Progress in *ab initio* nuclear structure and nuclear scattering

Unexpectedly large charge radii of neutron-rich calcium isotopes.

Garcia Ruiz *et al.*, Nature Phys. 12, 594 (2016).

Structure of ^{78}Ni from first principles computations.

Hagen, Jansen, & Papenbrock, PRL 117, 172501 (2016).

A nucleus-dependent valence-space approach to nuclear structure.

Stroberg *et al.*, PRL 118, 032502 (2017).

Ab initio many-body calculations of the $^3\text{H}(\text{d}, \text{n})^4\text{He}$ and $^3\text{He}(\text{d}, \text{p})^4\text{He}$ fusion.

Navratil & Quaglioni, PRL 108, 042503 (2012).

$^3\text{He}(\alpha, \gamma)^7\text{Be}$ and $^3\text{H}(\alpha, \gamma)^7\text{Li}$ astrophysical S factors from the no-core shell model with continuum Dohet-Eraly, J. *et al.* PLB B 757 (2016) 430-436.

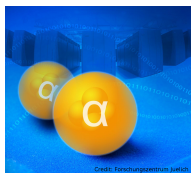
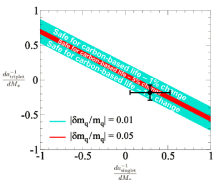
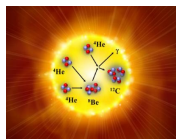
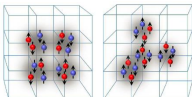
Elastic proton scattering of medium mass nuclei from coupled-cluster theory.

Hagen & Michel PRC 86, 021602 (2012).

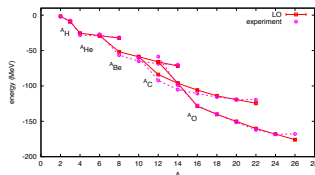
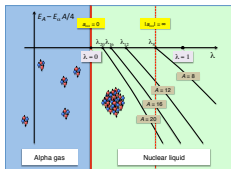
Coupling the Lorentz Integral Transform (LIT) and the Coupled Cluster (CC) Methods.

Orlandini, G. *et al.*, Few Body Syst. 55, 907-911 (2014).

Nuclear LEFT: *ab initio* nuclear structure and scattering theory

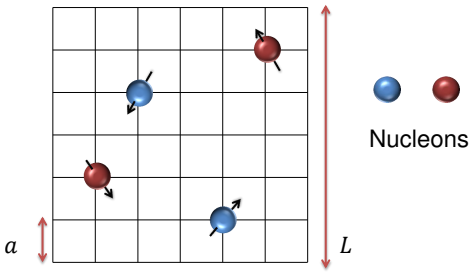


- Lattice EFT calculations for $A = 3, 4, 6, 12$ nuclei, [PRL 104 \(2010\) 142501](#)
- *Ab initio* calculation of the Hoyle state, [PRL 106 \(2011\) 192501](#)
- Structure and rotations of the Hoyle state, [PRL 109 \(2012\) 252501](#)
- Viability of Carbon-Based Life as a Function of the Light Quark Mass, [PRL 110 \(2013\) 112502](#)
- Radiative capture reactions in lattice effective field theory, [PRL 111 \(2013\) 032502](#)
- *Ab initio* calculation of the Spectrum and Structure of ^{16}O , [PRL 112 \(2014\) 102501](#)
- *Ab initio* alpha-alpha scattering, [Nature 528, 111-114 \(2015\)](#).
- Nuclear Binding Near a Quantum Phase Transition, [PRL 117, 132501 \(2016\)](#)
- *Ab initio* calculations of the isotopic dependence of nuclear clustering, [PRL 119, 222505 \(2017\)](#).



Lattice effective field theory

Lattice effective field theory is a powerful numerical method formulated in the framework of chiral effective field theory.



Nucleons

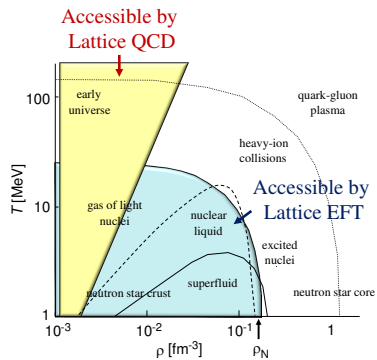


Fig. courtesy of D. Lee

Chiral EFT for nucleons: nuclear forces

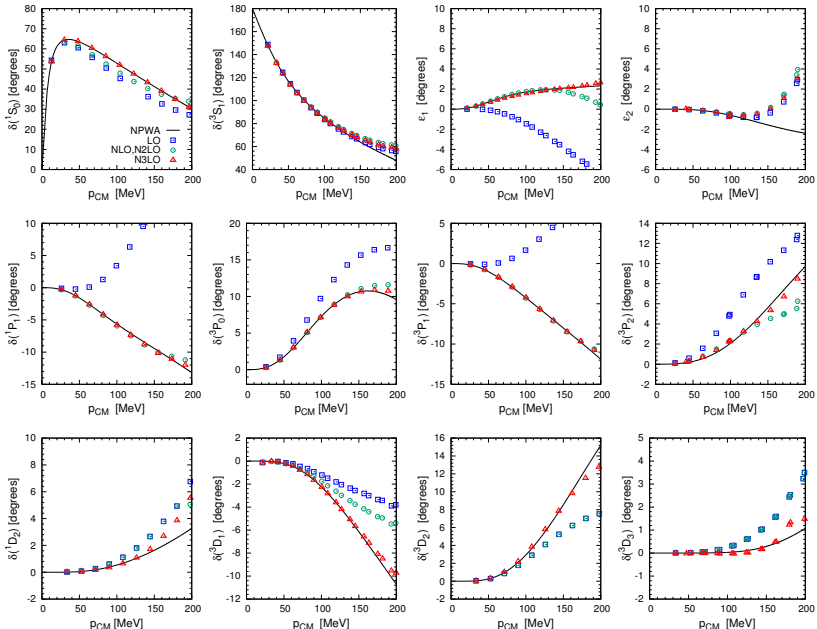
Chiral effective field theory organizes the nuclear interactions as an expansion in powers of momenta and other low energy scales such as the pion mass (Q/Λ_χ) .

	2N force	3N force	4N force
LO		—	—
NLO		—	—
N ² LO			—
N ³ LO			

Fig. courtesy of E.Epelbaum

Ordonez et al. '94; Friar & Coon '94; Kaiser et al. '97; Epelbaum et al. '98,'03,'05,'15; Kaiser '99-'01; Higa et al. '03; ...

Chiral EFT for nucleons: NN scattering phase shifts



Lattice Monte Carlo calculations

Transfer matrix operator formalism $\mathbf{M} = : \exp(-H a_t) :$

Microscopic Hamiltonian $H = H_{\text{free}} + V$

$$Z^{(L_t)} = \text{Tr}(\mathbf{M}^{L_t}) = \int Dc Dc^* \exp[-S(c, c^*)]$$

Creutz, Found. Phys. 30 (2000) 487.

The exact equivalence of several different lattice formulations.

Lee, PRC 78:024001, (2008); Prog.Part.Nucl.Phys., 63:117-154 (2009)

$$e^{-E_0 a_t} = \lim_{L_t \rightarrow \infty} Z^{(L_t+1)} / Z^{(L_t)}$$

These amplitudes are computed with the Hybrid Monte Carlo methods.

Phys. Lett. B195, 216-222 (1987), Phys. Rev. D35, 2531-2542 (1987).

Lattice Monte Carlo calculations

Nuclear forces posses approximate SU(4) symmetry. $H_{\text{SU}(4)}$ acts as an approximate and inexpensive low energy filter at few first/last time steps. Significant suppression of sign oscillations. [Chen, Lee, Schäfer, PRL 93 \(2004\) 242302](#)

$$|\psi_I(\tau')\rangle = [\mathbf{M}_{\text{SU}(4)}]^{L'_t} |\psi_I\rangle \quad \mathbf{M}_{\text{SU}(4)} = : e^{-a_t H_{\text{SU}(4)}} : \quad \tau' = L'_t a_t$$

For time steps in midsection, the full H_{LO} Hamiltonian is used.

$$|\psi_I(\tau)\rangle = [\mathbf{M}_{\text{LO}}]^{L_t} |\psi_I(\tau')\rangle \quad \mathbf{M}_{\text{LO}} = : e^{-a_t H_{\text{LO}}} : \quad \tau = L_t a_t$$

The ground state energy at LO can be extracted from

$$e^{-E_{\text{LO}} a_t} = \lim_{L_t \rightarrow \infty} \frac{Z_{\text{LO}}^{(L_t+1)}}{Z_{\text{LO}}^{(L_t)}} = \lim_{L_t \rightarrow \infty} \frac{\langle \psi_I(\tau/2) | \mathbf{M}_{\text{LO}} | \psi_I(\tau/2) \rangle}{\langle \psi_I(\tau/2) | \psi_I(\tau/2) \rangle}$$

Lattice Monte Carlo calculations

Higher order calculations (perturbative)

ho = NLO, NNLO, · · ·

$$\mathbf{M}_{\text{ho}} = : e^{-a_t(H_{\text{LO}} + V_{\text{ho}})} :$$

where the potential V_{ho} is treated perturbatively.

The higher order correction to the ground state energy can be extracted from

$$e^{-\Delta E_{\text{ho}} a_t} = \frac{Z_{\text{ho}}^{(L_t+1)}}{Z_{\text{LO}}^{(L_t+1)}} = \frac{\langle \psi_I(\tau/2) | \mathbf{M}_{\text{ho}} | \psi_I(\tau/2) \rangle}{\langle \psi_I(\tau/2) | \mathbf{M}_{\text{LO}} | \psi_I(\tau/2) \rangle}$$

Lattice Monte Carlo calculations

Compute observable \mathcal{O}

The observable \mathcal{O} at LO

$$\langle \mathcal{O} \rangle_{0,\text{LO}} = \lim_{L_t \rightarrow \infty} \frac{\langle \psi_I | [\mathbf{M}_{\text{LO}}]^{L_t} \mathcal{O} [\mathbf{M}_{\text{LO}}]^{L_t} | \psi_I \rangle}{\langle \psi_I | [\mathbf{M}_{\text{LO}}]^{2L_t+1} | \psi_I \rangle}$$

The observable \mathcal{O} at (NLO, NNLO, \dots)

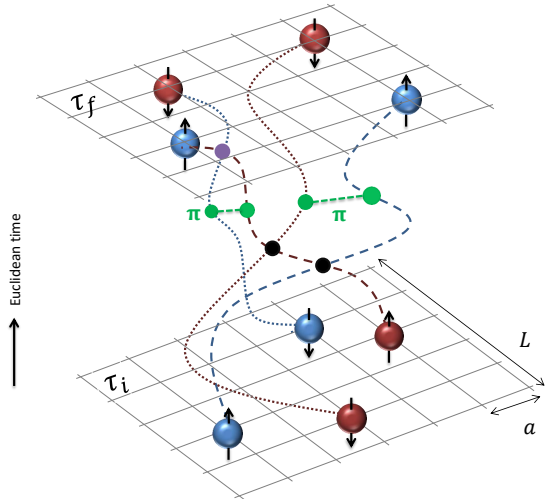
$$\langle \mathcal{O} \rangle_{0,\text{ho}} = \lim_{L_t \rightarrow \infty} \frac{\langle \psi_I | [\mathbf{M}_{\text{LO}}]^{L_t-1} \mathbf{M}_{\text{ho}} \mathcal{O} [\mathbf{M}_{\text{LO}}]^{L_t} | \psi_I \rangle}{\langle \psi_I | [\mathbf{M}_{\text{LO}}]^{L_t} \mathbf{M}_{\text{ho}} [\mathbf{M}_{\text{LO}}]^{L_t} | \psi_I \rangle}$$

Lattice EFT: (Euclidean time) projection Monte Carlo

$$e^{-H\tau}$$

$$\tau = L_t a_t$$

- evolve nucleons forward in Euclidean time
- allow them to interact

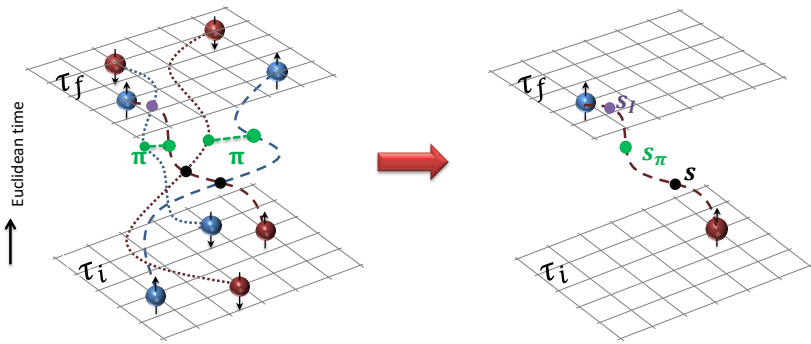


Auxiliary field Monte Carlo

Use a Gaussian integral identity

$$\exp \left[-\frac{C}{2} \left(N^\dagger N \right)^2 \right] = \sqrt{\frac{1}{2\pi}} \int ds \exp \left[-\frac{s^2}{2} + \sqrt{C} s \left(N^\dagger N \right) \right]$$

s is an auxiliary field coupled to particle density. Each nucleon evolves as if a single particle in a fluctuating background of pion fields and auxiliary fields.

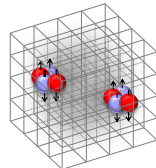


Adiabatic projection method

Scattering and reactions on the lattice

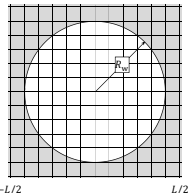
The first part

use Euclidean time projection to construct an *ab initio* low-energy cluster Hamiltonian, called the adiabatic Hamiltonian.



The second part

compute the two-cluster scattering phase shifts or reaction amplitudes using the adiabatic Hamiltonian.



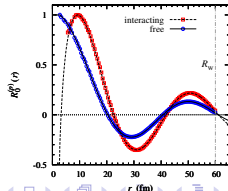
Rupak, Lee., PRL 111 (2013) 032502.

Pine, Lee, Rupak, EPJA 49 (2013) 151.

SE, Lee, PRC 90, 064001 (2014).

Rokash, Pine, SE, Lee, Epelbaum, Krebs, PRC 92,054612 (2015)

SE, Lee, Meißner, Rupak, EPJA 52: 174 (2016)

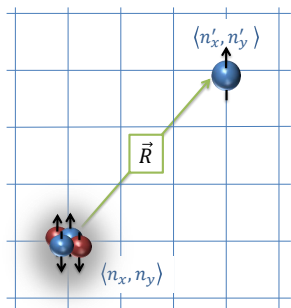


Adiabatic projection method

The method constructs a low energy effective theory for the clusters.

Use initial states parameterized by the relative spatial separation between clusters, and project them in Euclidean time.

$$|\vec{R}\rangle = \sum_{\vec{r}} |\vec{r} + \vec{R}\rangle_1 \otimes |\vec{r}\rangle_2$$



$$|\vec{R}\rangle_\tau = e^{-H\tau} |\vec{R}\rangle \quad \text{dressed cluster state}$$

The adiabatic projection in Euclidean time gives a systematically improvable description of the low-lying scattering cluster states.
In the limit of large Euclidean projection time the description becomes exact.

Adiabatic projection method

$$|\vec{R}\rangle_{\tau} = e^{-H\tau} |\vec{R}\rangle \quad \text{dressed cluster state (not orthogonal)}$$

Hamiltonian matrix

$$[H_{\tau}]_{\vec{R}, \vec{R}'} = {}_{\tau} \langle \vec{R} | H | \vec{R}' \rangle_{\tau}$$

Norm matrix

$$[N_{\tau}]_{\vec{R}, \vec{R}'} = {}_{\tau} \langle \vec{R} | \vec{R}' \rangle_{\tau}$$

$$[H_{\tau}^a]_{\vec{R}, \vec{R}'} = \sum_{\vec{R}'', \vec{R}'''} \left[N_{\tau}^{-1/2} \right]_{\vec{R} \vec{R}''} [H_{\tau}]_{\vec{R}'' \vec{R}'''} \left[N_{\tau}^{-1/2} \right]_{\vec{R}''' \vec{R}'}$$

The structure of the adiabatic Hamiltonian, $[H_{\tau}^a]_{\vec{R}, \vec{R}'}$, is similar to the Hamiltonian matrix used in calculations of ab initio no-core shell model/resonating group method (NCSM/RGM) for nuclear scattering and reactions.

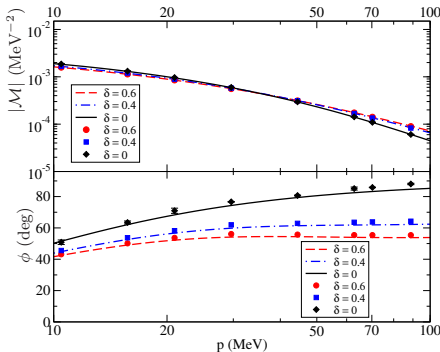
Navratil, Quaglioni, PRC 83, 044609 (2011).

Navratil, Roth, Quaglioni, PLB 704, 379 (2011).

Navratil, Quaglioni, PRL 108, 042503 (2012).

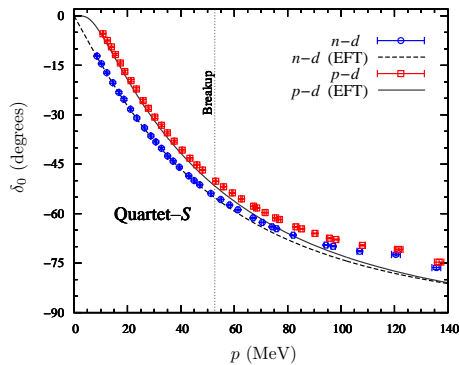
Adiabatic projection method

The radiative capture process $p(n, \gamma)d$.



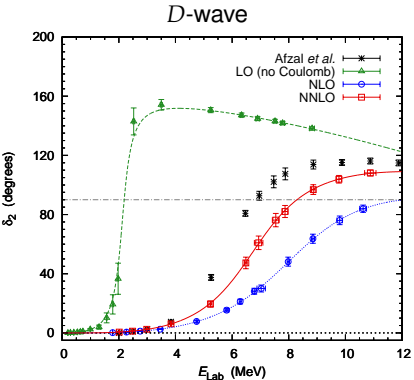
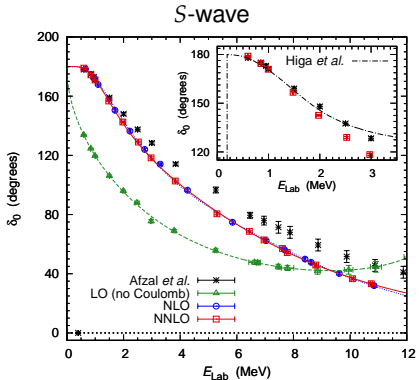
Rupak, Lee., PRL 111 (2013) 032502.

$N - d$ scattering.



SE, Lee, Meißner,Rupak. EPJ 52:174 (2016).

Alpha-alpha scattering



Afzal, Ahmad, Ali, Rev. Mod. Phys. 41, 247 (1969)

Higa, Hammer, van Kolck, Nucl.Phys. A809, 171 (2008)

SE, Lee, Rupak, Epelbaum, Krebs, Lähde, Luu, Meiñner, Nature 528, 111-114 (2015)

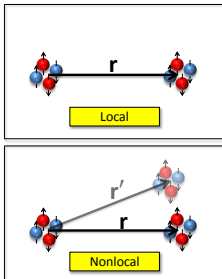
Degree of locality of nuclear forces

Interaction A

- Nonlocal short-range interactions $V(r, r')$
- One-pion exchange interaction
 - (+ Coulomb interaction)

Interaction B

- Local short-range interactions $V(r, r') = U(r)\delta(r - r')$
- Nonlocal short-range interactions $V(r, r')$
- One-pion exchange interaction
 - (+ Coulomb interaction)

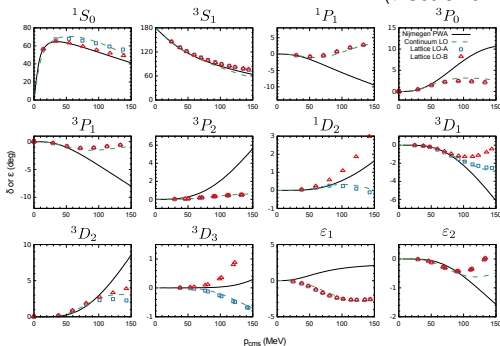


Introducing the nonlocal short-range interactions reduce the Monte Carlo sign oscillation significantly.

Degree of locality of nuclear forces

Interaction A

- Nonlocal short-range interactions $V(r, r')$
- One-pion exchange interaction
- (+ Coulomb interaction)

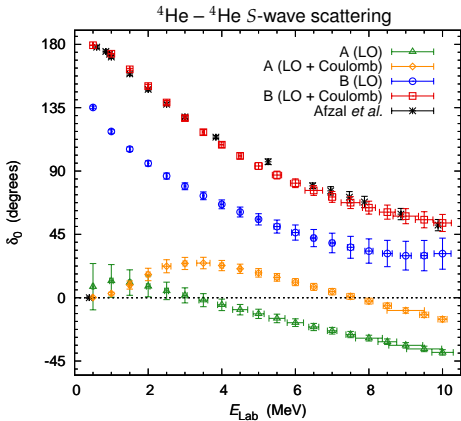


Interaction B

- Local short-range interactions $V(r, r') = U(r)\delta(r - r')$
- Nonlocal short-range interactions $V(r, r')$
- One-pion exchange interaction
- (+ Coulomb interaction)

Nucleus	A (LO)	B (LO)	A (LO + Coulomb)	B (LO + Coulomb)	Experiment
^3H	-7.82(5)	-7.78(12)	-7.82(5)	-7.78(12)	-8.482
^3He	-7.82(5)	-7.78(12)	-7.08(5)	-7.09(12)	-7.718
^4He	-29.36(4)	-29.19(6)	-28.62(4)	-28.45(6)	-28.296

Degree of locality of nuclear forces



Nucleus	A (LO)	B (LO)	A (LO + Coulomb)	B (LO + Coulomb)	Experiment
${}^8\text{Be}$	-58.61(14)	-59.73(6)	-56.51(14)	-57.29(7)	-56.591
${}^{12}\text{C}$	-88.2(3)	-95.0(5)	-84.0(3)	-89.9(5)	-92.162
${}^{16}\text{O}$	-117.5(6)	-135.4(7)	-110.5(6)	-126.0(7)	-127.619
${}^{20}\text{Ne}$	-148(1)	-178(1)	-137(1)	-164(1)	-160.645

Degree of locality of nuclear forces

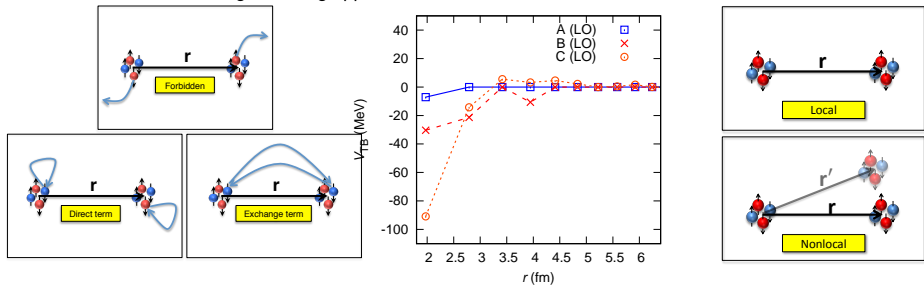
Interaction A

- Nonlocal short-range interactions $V(r, r')$
- One-pion exchange interaction
 - (+ Coulomb interaction)

Interaction B

- Local short-range interactions $V(r, r') = U(r)\delta(r - r')$
- Nonlocal short-range interactions $V(r, r')$
- One-pion exchange interaction
 - (+ Coulomb interaction)

Tight-binding approximation



The alpha-alpha interaction is sensitive to the degree of locality of the interaction.

Nuclear binding near a quantum phase transition

Nucleus	A (LO)	B (LO)	A (LO + Coulomb)	B (LO + Coulomb)	Experiment
^4He	-29.36(4)	-29.19(6)	-28.62(4)	-28.45(6)	-28.296
^8Be	-58.61(14)	-59.73(6)	-56.51(14)	-57.29(7)	-56.591
^{12}C	-88.2(3)	-95.0(5)	-84.0(3)	-89.9(5)	-92.162
^{16}O	-117.5(6)	-135.4(7)	-110.5(6)	-126.0(7)	-127.619
^{20}Ne	-148(1)	-178(1)	-137(1)	-164(1)	-160.645

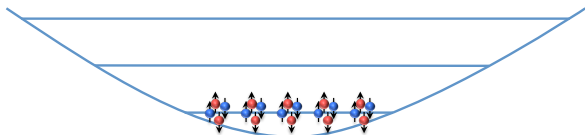
$$\frac{E_{^8\text{Be}}}{E_{^4\text{He}}} = 1.997(6)$$

$$\frac{E_{^{12}\text{C}}}{E_{^4\text{He}}} = 3.00(1)$$

$$\frac{E_{^{16}\text{O}}}{E_{^4\text{He}}} = 4.00(2)$$

$$\frac{E_{^{20}\text{Ne}}}{E_{^4\text{He}}} = 5.03(3)$$

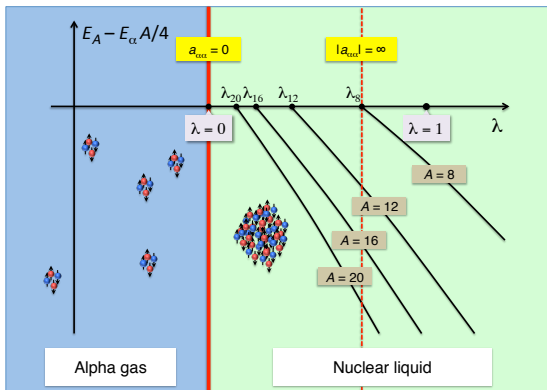
Bose condensate of alpha particles!



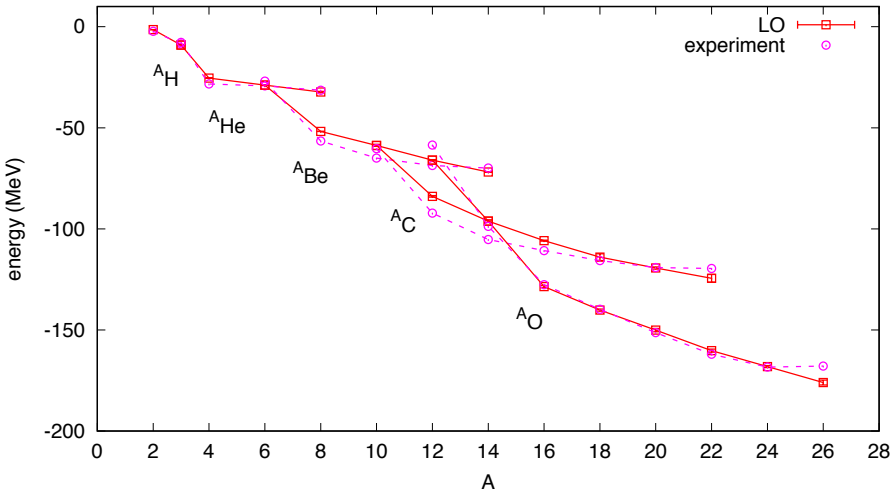
Nuclear binding near a quantum phase transition

Nucleus	A (LO)	B (LO)	A (LO + Coulomb)	B (LO + Coulomb)	Experiment
^4He	-29.36(4)	-29.19(6)	-28.62(4)	-28.45(6)	-28.296
^8Be	-58.61(14)	-59.73(6)	-56.51(14)	-57.29(7)	-56.591
^{12}C	-88.2(3)	-95.0(5)	-84.0(3)	-89.9(5)	-92.162
^{16}O	-117.5(6)	-135.4(7)	-110.5(6)	-126.0(7)	-127.619
^{20}Ne	-148(1)	-178(1)	-137(1)	-164(1)	-160.645

$$V = (1 - \lambda)V_A + \lambda V_B$$



Ground state energies at LO



SE, Epelbaum, Krebs, Lähde, Lee, Li, Lu, Meißner, Rupak, PRL 119, 222505 (2017)

Nuclear clusters: probing for alpha clusters

$\rho(\vec{n})$: the total nucleon density operator on the lattice site \vec{n} .

$\rho_4 = \sum_{\vec{n}} : \rho^4(\vec{n}) / 4! :$ is defined to construct a probe for alpha clusters.

Similarly ρ_3 is to construct a second probe for alpha clusters only in nuclei with even Z and even N where ${}^3\text{H}$ and ${}^3\text{He}$ clusters are not energetically favorable.

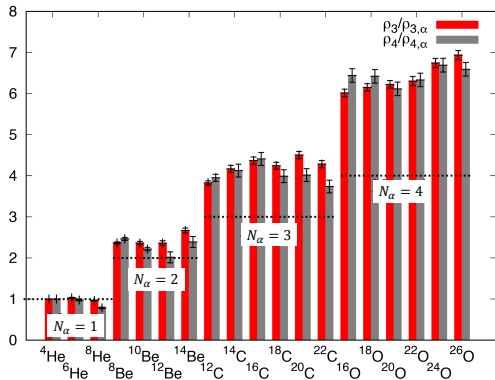
$$\rho_3 = \sum_{\vec{n}} : \rho^3(\vec{n}) / 3! :$$

ρ_3 and ρ_4 depend on the short-distance regulator, the lattice spacing a . However the regularization-scale dependence of ρ_3 and ρ_4 does not depend on the nucleus being considered.

Therefore, by defining $\rho_{3,\alpha}$ and $\rho_{4,\alpha}$ as the corresponding values for the alpha particle, we consider the ratios $\rho_3/\rho_{3,\alpha}$ and $\rho_4/\rho_{4,\alpha}$ that are free from short-distance divergences and are model-independent quantities up to contributions from higher-dimensional operators in an operator product expansion.

Nuclear clusters: probing for alpha clusters

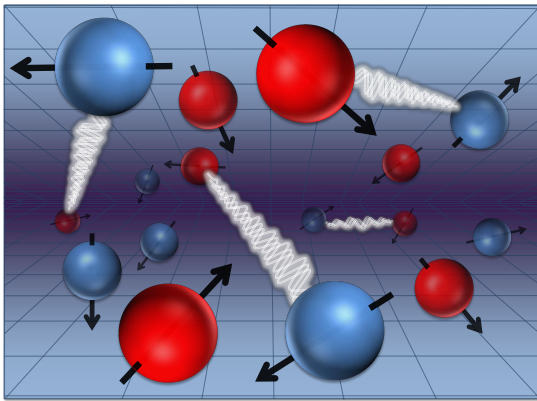
$\Delta_\alpha^{\rho_3} / N_\alpha$ the ρ_3 -entanglement of the alpha clusters ,
where $\Delta_\alpha^{\rho_3} = \rho_3 / \rho_{3,\alpha} - N_\alpha$.



Nucleus	${}^{4,6,8}\text{He}$	${}^{8,10,12,14}\text{Be}$	${}^{12,14,16,18,20,22}\text{C}$	${}^{16,18,20,22,24,26,28}\text{O}$
$\Delta_\alpha^{\rho_3} / N_\alpha$	0.0 – 0.03	0.20 – 0.35	0.25 – 0.50	0.50 – 0.75

Nuclear clusters: probing for alpha clusters

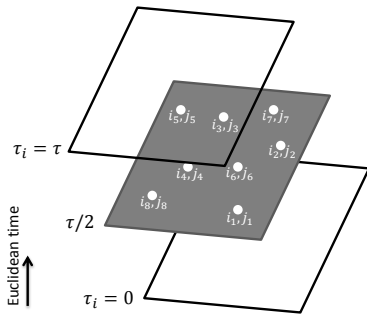
Our results show that the transition from cluster-like states in light systems to nuclear liquid-like states in heavier systems should not be viewed as a simple suppression of multi-nucleon short-distance correlations, but rather an increasing entanglement of the nucleons involved in the multi-nucleon correlations.



Density profiles for nuclei: pinhole algorithm

The simulations with auxiliary-field Monte Carlo methods involve quantum states that are superposition of many different center-of-mass positions. Therefore, the density distributions of the nucleons cannot be computed directly.

Consider a screen placed at the middle time step having pinholes with spin and isospin labels that allow nucleons with the corresponding spin and isospin to pass.



Density profiles for nuclei: pinhole algorithm

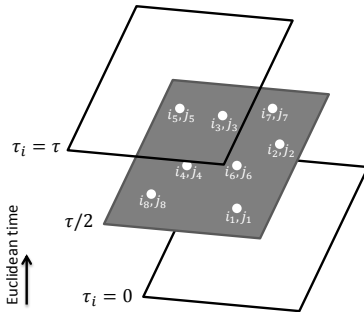
This opaque screen corresponds to the insertion of the normal-ordered A -body density operator,

$$\rho_{i_1, j_1, \dots, i_A, j_A}(\vec{n}_1, \dots, \vec{n}_A) = : \rho_{i_1, j_1}(\vec{n}_1) \dots \rho_{i_A, j_A}(\vec{n}_A) :$$

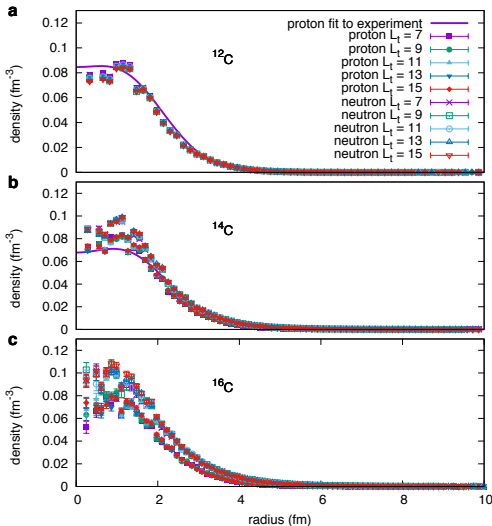
where $\rho_{i,j}(\vec{n}) = a_{i,j}^\dagger(\vec{n})a_{i,j}(\vec{n})$ is the density operator for nucleon with spin i and isospin j .

We perform Monte Carlo sampling of the amplitude,

$$A_{i_1, j_1, \dots, i_A, j_A}(\vec{n}_1, \dots, \vec{n}_A, L_t) = \langle \psi_I(\tau) | \rho_{i_1, j_1, \dots, i_A, j_A}(\vec{n}_1, \dots, \vec{n}_A) | \psi_I(\tau) \rangle$$



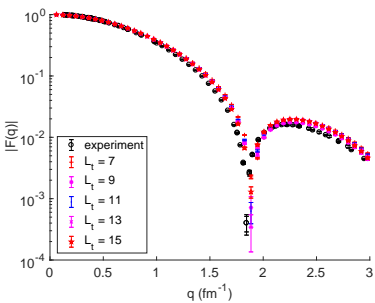
Pinhole algorithm: proton and neutron densities



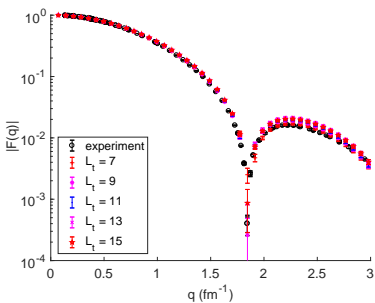
SE, Epelbaum, Krebs, Lähde, Lee, Li, Lu, Meißner, Rupak, PRL 119, 222505 (2017)

Pinhole algorithm: ^{12}C and ^{14}C electric form factor

The magnitude of the ^{12}C electric form factor



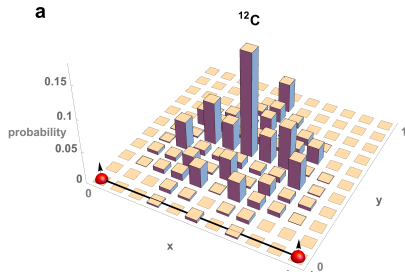
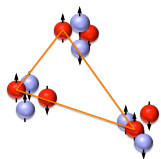
The magnitude of the ^{14}C electric form factor



SE, Epelbaum, Krebs, Lähde, Lee, Li, Lu, Meißner, Rupak, PRL 119, 222505 (2017)

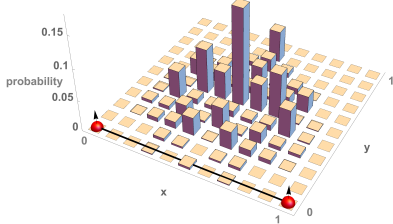
Pinhole algorithm: measure of alpha cluster geometry

Consider the triangular shape formed by the three spin-up protons.



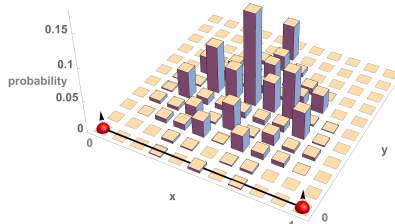
b

^{14}C



c

^{16}C



Summary

Scattering and reaction processes involving alpha particle are in reach of *ab initio* methods and this has opened the door towards using experimental data from collisions of heavier nuclei as input to improve *ab initio* nuclear structure theory.

Understanding of the connection between the degree of locality of nuclear forces and nuclear structure has led to a more efficient set of lattice chiral EFT interactions (to be proven by the higher order corrections).

The pinhole algorithm has been developed for the auxiliary-field Monte Carlo methods for the calculation of arbitrary density correlations with respect to the center of mass.

Thanks!

Extras